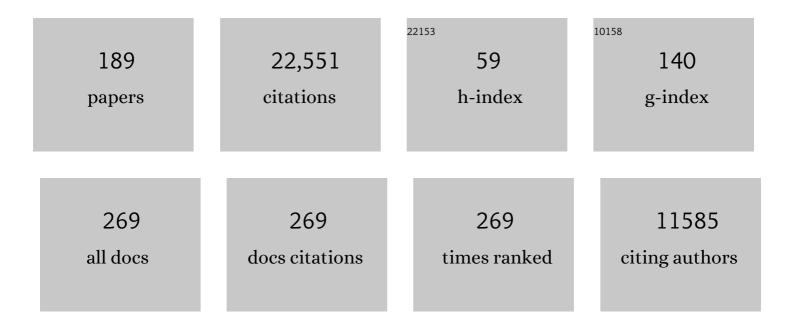
Kelly Chance

List of Publications by Year in descending order

Source: https://exaly.com/author-pdf/5908040/publications.pdf Version: 2024-02-01



#	Article	IF	CITATIONS
1	The HITRAN 2008 molecular spectroscopic database. Journal of Quantitative Spectroscopy and Radiative Transfer, 2009, 110, 533-572.	2.3	3,129
2	The HITRAN2012 molecular spectroscopic database. Journal of Quantitative Spectroscopy and Radiative Transfer, 2013, 130, 4-50.	2.3	2,810
3	The HITRAN 2004 molecular spectroscopic database. Journal of Quantitative Spectroscopy and Radiative Transfer, 2005, 96, 139-204.	2.3	2,601
4	The HITRAN molecular spectroscopic database: edition of 2000 including updates through 2001. Journal of Quantitative Spectroscopy and Radiative Transfer, 2003, 82, 5-44.	2.3	1,080
5	Global inventory of nitrogen oxide emissions constrained by space-based observations of NO2columns. Journal of Geophysical Research, 2003, 108, .	3.3	442
6	Global partitioning of NOx sources using satellite observations: Relative roles of fossil fuel combustion, biomass burning and soil emissions. Faraday Discussions, 2005, 130, 407.	3.2	392
7	Ring effect studies: Rayleigh scattering, including molecular parameters for rotational Raman scattering, and the Fraunhofer spectrum. Applied Optics, 1997, 36, 5224.	2.1	366
8	An improved retrieval of tropospheric nitrogen dioxide from GOME. Journal of Geophysical Research, 2002, 107, ACH 9-1.	3.3	355
9	Mapping isoprene emissions over North America using formaldehyde column observations from space. Journal of Geophysical Research, 2003, 108, .	3.3	346
10	An improved high-resolution solar reference spectrum for earth's atmosphere measurements in the ultraviolet, visible, and near infrared. Journal of Quantitative Spectroscopy and Radiative Transfer, 2010, 111, 1289-1295.	2.3	346
11	Air mass factor formulation for spectroscopic measurements from satellites: Application to formaldehyde retrievals from the Global Ozone Monitoring Experiment. Journal of Geophysical Research, 2001, 106, 14539-14550.	3.3	318
12	The Ozone Monitoring Instrument: overview of 14 years in space. Atmospheric Chemistry and Physics, 2018, 18, 5699-5745.	4.9	259
13	Ozone profile retrievals from the Ozone Monitoring Instrument. Atmospheric Chemistry and Physics, 2010, 10, 2521-2537.	4.9	250
14	Quantifying the seasonal and interannual variability of North American isoprene emissions using satellite observations of the formaldehyde column. Journal of Geophysical Research, 2006, 111, .	3.3	240
15	Tropospheric emissions: Monitoring of pollution (TEMPO). Journal of Quantitative Spectroscopy and Radiative Transfer, 2017, 186, 17-39.	2.3	239
16	Spatial distribution of isoprene emissions from North America derived from formaldehyde column measurements by the OMI satellite sensor. Journal of Geophysical Research, 2008, 113, .	3.3	234
17	Application of satellite observations for timely updates to global anthropogenic NO _{<i>x</i>} emission inventories. Geophysical Research Letters, 2011, 38, n/a-n/a.	4.0	234
18	Space-based formaldehyde measurements as constraints on volatile organic compound emissions in east and south Asia and implications for ozone. Journal of Geophysical Research, 2007, 112, .	3.3	232

#	Article	IF	CITATIONS
19	Satellite observations of atmospheric methane and their value for quantifying methane emissions. Atmospheric Chemistry and Physics, 2016, 16, 14371-14396.	4.9	230
20	Satellite observations of formaldehyde over North America from GOME. Geophysical Research Letters, 2000, 27, 3461-3464.	4.0	218
21	Sensitivity of ozone to bromine in the lower stratosphere. Geophysical Research Letters, 2005, 32, .	4.0	207
22	Evaluation of space-based constraints on global nitrogen oxide emissions with regional aircraft measurements over and downwind of eastern North America. Journal of Geophysical Research, 2006, 111, .	3.3	181
23	Ozone profile and tropospheric ozone retrievals from the Global Ozone Monitoring Experiment: Algorithm description and validation. Journal of Geophysical Research, 2005, 110, .	3.3	171
24	Analysis of BrO measurements from the Global Ozone Monitoring Experiment. Geophysical Research Letters, 1998, 25, 3335-3338.	4.0	167
25	Isoprene emissions in Africa inferred from OMI observations of formaldehyde columns. Atmospheric Chemistry and Physics, 2012, 12, 6219-6235.	4.9	166
26	Evaluating a Spaceâ€Based Indicator of Surface Ozoneâ€NO _{<i>x</i>} â€VOC Sensitivity Over Midlatitude Source Regions and Application to Decadal Trends. Journal of Geophysical Research D: Atmospheres, 2017, 122, 10-461.	3.3	165
27	New Era of Air Quality Monitoring from Space: Geostationary Environment Monitoring Spectrometer (GEMS). Bulletin of the American Meteorological Society, 2020, 101, E1-E22.	3.3	165
28	The GEISA spectroscopic database: Current and future archive for Earth and planetary atmosphere studies. Journal of Quantitative Spectroscopy and Radiative Transfer, 2008, 109, 1043-1059.	2.3	161
29	Remote sensed and in situ constraints on processes affecting tropical tropospheric ozone. Atmospheric Chemistry and Physics, 2007, 7, 815-838.	4.9	156
30	Updated Smithsonian Astrophysical Observatory Ozone Monitoring Instrument (SAO OMI) formaldehyde retrieval. Atmospheric Measurement Techniques, 2015, 8, 19-32.	3.1	142
31	Constraining global isoprene emissions with Global Ozone Monitoring Experiment (GOME) formaldehyde column measurements. Journal of Geophysical Research, 2005, 110, .	3.3	140
32	Satellite mapping of rain-induced nitric oxide emissions from soils. Journal of Geophysical Research, 2004, 109, n/a-n/a.	3.3	137
33	Formaldehyde (HCHO) As a Hazardous Air Pollutant: Mapping Surface Air Concentrations from Satellite and Inferring Cancer Risks in the United States. Environmental Science & Technology, 2017, 51, 5650-5657.	10.0	131
34	Seasonal and interannual variability of North American isoprene emissions as determined by formaldehyde column measurements from space. Geophysical Research Letters, 2003, 30, n/a-n/a.	4.0	125
35	The United States' Next Generation of Atmospheric Composition and Coastal Ecosystem Measurements: NASA's Geostationary Coastal and Air Pollution Events (GEO-CAPE) Mission. Bulletin of the American Meteorological Society, 2012, 93, 1547-1566.	3.3	118
36	A new interpretation of total column BrO during Arctic spring. Geophysical Research Letters, 2010, 37,	4.0	116

#	Article	IF	CITATIONS
37	Evaluation of GOME satellite measurements of tropospheric NO2and HCHO using regional data from aircraft campaigns in the southeastern United States. Journal of Geophysical Research, 2004, 109, .	3.3	113
38	Remote Sensing of Tropospheric Pollution from Space. Bulletin of the American Meteorological Society, 2008, 89, 805-822.	3.3	108
39	Intercomparison methods for satellite measurements of atmospheric composition: application to tropospheric ozone from TES and OMI. Atmospheric Chemistry and Physics, 2010, 10, 4725-4739.	4.9	106
40	Application of OMI, SCIAMACHY, and GOMEâ€2 satellite SO ₂ retrievals for detection of large emission sources. Journal of Geophysical Research D: Atmospheres, 2013, 118, 11,399.	3.3	102
41	Net ecosystem fluxes of isoprene over tropical South America inferred from Global Ozone Monitoring Experiment (GOME) observations of HCHO columns. Journal of Geophysical Research, 2008, 113, .	3.3	99
42	Observing atmospheric formaldehyde (HCHO) from space: validation and intercomparison of six retrievals from four satellites (OMI, GOME2A, GOME2B, OMPS) with SEAC ⁴ RS aircraft observations over the southeast US. Atmospheric Chemistry and Physics, 2016, 16, 13477-13490.	4.9	99
43	Satellite observation of lowermost tropospheric ozone by multispectral synergism of IASI thermal infrared and GOME-2 ultraviolet measurements over Europe. Atmospheric Chemistry and Physics, 2013, 13, 9675-9693.	4.9	97
44	Evidence of lightning NOxand convective transport of pollutants in satellite observations over North America. Geophysical Research Letters, 2005, 32, .	4.0	95
45	Anthropogenic emissions of highly reactive volatile organic compounds in eastern Texas inferred from oversampling of satellite (OMI) measurements of HCHO columns. Environmental Research Letters, 2014, 9, 114004.	5.2	95
46	Estimating European volatile organic compound emissions using satellite observations of formaldehyde from the Ozone Monitoring Instrument. Atmospheric Chemistry and Physics, 2010, 10, 11501-11517.	4.9	94
47	A numerical testbed for remote sensing of aerosols, and its demonstration for evaluating retrieval synergy from a geostationary satellite constellation of GEO-CAPE and GOES-R. Journal of Quantitative Spectroscopy and Radiative Transfer, 2014, 146, 510-528.	2.3	94
48	The formaldehyde budget as seen by a global-scale multi-constraint and multi-species inversion system. Atmospheric Chemistry and Physics, 2012, 12, 6699-6721.	4.9	93
49	Improved tropospheric ozone profile retrievals using OMI and TES radiances. Geophysical Research Letters, 2007, 34, .	4.0	85
50	Topâ€down isoprene emissions over tropical South America inferred from SCIAMACHY and OMI formaldehyde columns. Journal of Geophysical Research D: Atmospheres, 2013, 118, 6849-6868.	3.3	84
51	First observations of iodine oxide from space. Geophysical Research Letters, 2007, 34, .	4.0	83
52	Ultraviolet and visible absorption cross-sections for HITRAN. Journal of Quantitative Spectroscopy and Radiative Transfer, 2003, 82, 491-504.	2.3	81
53	Improved algorithm for MODIS satellite retrievals of aerosol optical depths over western North America. Journal of Geophysical Research, 2008, 113, .	3.3	77
54	Validation of Ozone Monitoring Instrument (OMI) ozone profiles and stratospheric ozone columns with Microwave Limb Sounder (MLS) measurements. Atmospheric Chemistry and Physics, 2010, 10, 2539-2549.	4.9	77

#	Article	IF	CITATIONS
55	Retrievals of sulfur dioxide from the Global Ozone Monitoring Experiment 2 (GOME-2) using an optimal estimation approach: Algorithm and initial validation. Journal of Geophysical Research, 2011, 116, .	3.3	74
56	Anthropogenic emissions in Nigeria and implications for atmospheric ozone pollution: A view from space. Atmospheric Environment, 2014, 99, 32-40.	4.1	73
57	Glyoxal yield from isoprene oxidation and relation to formaldehyde: chemical mechanism, constraints from SENEX aircraft observations, and interpretation of OMI satellite data. Atmospheric Chemistry and Physics, 2017, 17, 8725-8738.	4.9	72
58	Undersampling correction for array detector-based satellite spectrometers. Applied Optics, 2005, 44, 1296.	2.1	71
59	Latitudinal and vertical distribution of bromine monoxide in the lower stratosphere from Scanning Imaging Absorption Spectrometer for Atmospheric Chartography limb scattering measurements. Journal of Geophysical Research, 2006, 111, .	3.3	70
60	Longâ€ŧerm (2005–2014) trends in formaldehyde (HCHO) columns across North America as seen by the OMI satellite instrument: Evidence of changing emissions of volatile organic compounds. Geophysical Research Letters, 2017, 44, 7079-7086.	4.0	68
61	Glyoxal retrieval from the Ozone Monitoring Instrument. Atmospheric Measurement Techniques, 2014, 7, 3891-3907.	3.1	67
62	Global satellite analysis of the relation between aerosols and short-lived trace gases. Atmospheric Chemistry and Physics, 2011, 11, 1255-1267.	4.9	65
63	Revisiting the effectiveness of HCHO/NO2 ratios for inferring ozone sensitivity to its precursors using high resolution airborne remote sensing observations in a high ozone episode during the KORUS-AQ campaign. Atmospheric Environment, 2020, 224, 117341.	4.1	65
64	A physics-based approach to oversample multi-satellite, multispecies observations to a common grid. Atmospheric Measurement Techniques, 2018, 11, 6679-6701.	3.1	64
65	Detection of biomass burning combustion products in Southeast Asia from backscatter data taken by the GOME Spectrometer. Geophysical Research Letters, 1998, 25, 1317-1320.	4.0	63
66	Analysis of satellite-derived Arctic tropospheric BrO columns in conjunction with aircraft measurements during ARCTAS and ARCPAC. Atmospheric Chemistry and Physics, 2012, 12, 1255-1285.	4.9	63
67	First directly retrieved global distribution of tropospheric column ozone from GOME: Comparison with the GEOS-CHEM model. Journal of Geophysical Research, 2006, 111, .	3.3	61
68	Ozone air quality measurement requirements for a geostationary satellite mission. Atmospheric Environment, 2011, 45, 7143-7150.	4.1	61
69	Global ozone–CO correlations from OMI and AIRS: constraints on tropospheric ozone sources. Atmospheric Chemistry and Physics, 2013, 13, 9321-9335.	4.9	60
70	Multi-spectral sensitivity studies for the retrieval of tropospheric and lowermost tropospheric ozone from simulated clear-sky GEO-CAPE measurements. Atmospheric Environment, 2011, 45, 7151-7165.	4.1	59
71	Potential of next-generation imaging spectrometers to detect and quantify methane point sources from space. Atmospheric Measurement Techniques, 2019, 12, 5655-5668.	3.1	58
72	SCIAMACHY Level 1 data: calibration concept and in-flight calibration. Atmospheric Chemistry and Physics, 2006, 6, 5347-5367.	4.9	57

#	Article	IF	CITATIONS
73	Tropospheric emissions: monitoring of pollution (TEMPO). Proceedings of SPIE, 2013, , .	0.8	57
74	Absorption cross-sections of ozone in the ultraviolet and visible spectral regions: Status report 2015. Journal of Molecular Spectroscopy, 2016, 327, 105-121.	1.2	57
75	Stratospheric profiles of nitrogen dioxide observed by Optical Spectrograph and Infrared Imager System on the Odin satellite. Journal of Geophysical Research, 2003, 108, .	3.3	56
76	Springtime transitions of NO ₂ , CO, and O ₃ over North America: Model evaluation and analysis. Journal of Geophysical Research, 2008, 113, .	3.3	56
77	Formaldehyde columns from the Ozone Monitoring Instrument: Urban versus background levels and evaluation using aircraft data and a global model. Journal of Geophysical Research, 2011, 116, .	3.3	56
78	Evaluation of AIRS, IASI, and OMI ozone profile retrievals in the extratropical tropopause region using in situ aircraft measurements. Journal of Geophysical Research, 2009, 114, .	3.3	55
79	Characterization and correction of Global Ozone Monitoring Experiment 2 ultraviolet measurements and application to ozone profile retrievals. Journal of Geophysical Research, 2012, 117, .	3.3	55
80	Widespread persistent near-surface ozone depletion at northern high latitudes in spring. Geophysical Research Letters, 2003, 30, .	4.0	53
81	Impact of using different ozone cross sections on ozone profile retrievals from Global Ozone Monitoring Experiment (GOME) ultraviolet measurements. Atmospheric Chemistry and Physics, 2007, 7, 3571-3578.	4.9	53
82	Impact of very short-lived halogens on stratospheric ozone abundance and UV radiation in a geo-engineered atmosphere. Atmospheric Chemistry and Physics, 2012, 12, 10945-10955.	4.9	53
83	Validation of 10-year SAO OMI Ozone Profile (PROFOZ) product using ozonesonde observations. Atmospheric Measurement Techniques, 2017, 10, 2455-2475.	3.1	53
84	The TSISâ€1 Hybrid Solar Reference Spectrum. Geophysical Research Letters, 2021, 48, e2020GL091709.	4.0	53
85	Improved model of isoprene emissions in Africa using Ozone Monitoring Instrument (OMI) satellite observations of formaldehyde: implications for oxidants and particulate matter. Atmospheric Chemistry and Physics, 2014, 14, 7693-7703.	4.9	52
86	The unique OMI HCHO/NO2 feature during the 2008 Beijing Olympics: Implications for ozone production sensitivity. Atmospheric Environment, 2011, 45, 3103-3111.	4.1	50
87	Nitrogen dioxide observations from the Geostationary Trace gas and Aerosol Sensor Optimization (GeoTASO) airborne instrument: Retrieval algorithm and measurements during DISCOVER-AQ Texas 2013. Atmospheric Measurement Techniques, 2016, 9, 2647-2668.	3.1	50
88	Long-term tropospheric formaldehyde concentrations deduced from ground-based fourier transform solar infrared measurements. Atmospheric Chemistry and Physics, 2009, 9, 7131-7142.	4.9	49
89	Smithsonian Astrophysical Observatory Ozone Mapping and Profiler Suite (SAO OMPS) formaldehyde retrieval. Atmospheric Measurement Techniques, 2016, 9, 2797-2812.	3.1	48
90	Can a "state of the art―chemistry transport model simulate Amazonian tropospheric chemistry?. Journal of Geophysical Research, 2011, 116, .	3.3	47

#	Article	IF	CITATIONS
91	Hotspot of glyoxal over the Pearl River delta seen from the OMI satellite instrument: implications for emissions of aromatic hydrocarbons. Atmospheric Chemistry and Physics, 2016, 16, 4631-4639.	4.9	47
92	Adjoint inversion of Chinese non-methane volatile organic compound emissions using space-based observations of formaldehyde and glyoxal. Atmospheric Chemistry and Physics, 2018, 18, 15017-15046.	4.9	46
93	Stratospheric and tropospheric NO2 observed by SCIAMACHY: first results. Advances in Space Research, 2004, 34, 780-785.	2.6	44
94	Characteristics of tropospheric ozone depletion events in the Arctic spring: analysis of the ARCTAS, ARCPAC, and ARCIONS measurements and satellite BrO observations. Atmospheric Chemistry and Physics, 2012, 12, 9909-9922.	4.9	42
95	Monitoring Air Quality from Space: The Case for the Geostationary Platform. Bulletin of the American Meteorological Society, 2012, 93, 221-233.	3.3	41
96	Halogen-driven low-altitude O3and hydrocarbon losses in spring at northern high latitudes. Journal of Geophysical Research, 2006, 111, .	3.3	40
97	Water vapor retrieval from OMI visible spectra. Atmospheric Measurement Techniques, 2014, 7, 1901-1913.	3.1	40
98	Monitoring high-ozone events in the US Intermountain West using TEMPO geostationary satellite observations. Atmospheric Chemistry and Physics, 2014, 14, 6261-6271.	4.9	40
99	The smithsonian astrophysical observatory database SAO92. Journal of Quantitative Spectroscopy and Radiative Transfer, 1994, 52, 447-457.	2.3	39
100	Nitrogen dioxide and formaldehyde measurements from the GEOstationary Coastal and Air Pollution Events (GEO-CAPE) Airborne Simulator over Houston, Texas. Atmospheric Measurement Techniques, 2018, 11, 5941-5964.	3.1	39
101	Evaluation of Global Ozone Monitoring Experiment (GOME) ozone profiles from nine different algorithms. Journal of Geophysical Research, 2006, 111, .	3.3	38
102	Tropospheric ozone column retrieval at northern mid-latitudes from the Ozone Monitoring Instrument by means of a neural network algorithm. Atmospheric Measurement Techniques, 2011, 4, 2375-2388.	3.1	38
103	The role of OH production in interpreting the variability of CH ₂ O columns in the southeast U.S Journal of Geophysical Research D: Atmospheres, 2016, 121, 478-493.	3.3	38
104	Revised ultraviolet absorption cross sections of H2CO for the HITRAN database. Journal of Quantitative Spectroscopy and Radiative Transfer, 2011, 112, 1509-1510.	2.3	37
105	Evaluation of ozone profile and tropospheric ozone retrievals from GEMS and OMI spectra. Atmospheric Measurement Techniques, 2013, 6, 239-249.	3.1	36
106	An optimal-estimation-based aerosol retrieval algorithm using OMI near-UV observations. Atmospheric Chemistry and Physics, 2016, 16, 177-193.	4.9	35
107	Tibetan middle tropospheric ozone minimum in June discovered from GOME observations. Geophysical Research Letters, 2009, 36, .	4.0	34
108	Correction to "First directly retrieved global distribution of tropospheric column ozone from GOME: Comparison with the GEOS-CHEM model― Journal of Geophysical Research, 2006, 111, n/a-n/a.	3.3	33

#	Article	IF	CITATIONS
109	Intercomparison of GOME, ozonesonde, and SAGE II measurements of ozone: Demonstration of the need to homogenize available ozonesonde data sets. Journal of Geophysical Research, 2006, 111, .	3.3	31
110	Assessing sources of uncertainty in formaldehyde air mass factors over tropical South America: Implications for topâ€down isoprene emission estimates. Journal of Geophysical Research, 2012, 117, .	3.3	31
111	Characterization and correction of OMPS nadir mapper measurements for ozone profile retrievals. Atmospheric Measurement Techniques, 2017, 10, 4373-4388.	3.1	31
112	An inversion of NO _{<i>x</i>} and non-methane volatile organic compound (NMVOC) emissions using satellite observations during the KORUS-AQ campaign and implications for surface ozone over East Asia. Atmospheric Chemistry and Physics, 2020, 20, 9837-9854.	4.9	30
113	Improvement of OMI ozone profile retrievals in the upper troposphere and lower stratosphere by the use of a tropopause-based ozone profile climatology. Atmospheric Measurement Techniques, 2013, 6, 2239-2254.	3.1	29
114	Improved ozone profile retrievals from GOME data with degradation correction in reflectance. Atmospheric Chemistry and Physics, 2007, 7, 1575-1583.	4.9	28
115	Improved monitoring of surface ozone by joint assimilation of geostationary satellite observations of ozone and CO. Atmospheric Environment, 2014, 84, 254-261.	4.1	28
116	Validation of OMI HCHO data and its analysis over Asia. Science of the Total Environment, 2014, 490, 93-105.	8.0	28
117	Validation of OMI total ozone retrievals from the SAO ozone profile algorithm and three operational algorithms with Brewer measurements. Atmospheric Chemistry and Physics, 2015, 15, 667-683.	4.9	28
118	The impact of local surface changes in Borneo on atmospheric composition at wider spatial scales: coastal processes, land-use change and air quality. Philosophical Transactions of the Royal Society B: Biological Sciences, 2011, 366, 3210-3224.	4.0	27
119	Characterization of soluble bromide measurements and a case study of BrO observations during ARCTAS. Atmospheric Chemistry and Physics, 2012, 12, 1327-1338.	4.9	27
120	Characterization and verification of ACAM slit functions for trace-gas retrievals during the 2011 DISCOVER-AQ flight campaign. Atmospheric Measurement Techniques, 2015, 8, 751-759.	3.1	27
121	Preliminary results for HCHO and BrO from the EOS-Aura Ozone Monitoring Instrument. , 2004, , .		26
122	Five decades observing Earth's atmospheric trace gases using ultraviolet and visible backscatter solar radiation from space. Journal of Quantitative Spectroscopy and Radiative Transfer, 2019, 238, 106478.	2.3	26
123	Unraveling pathways of elevated ozone induced by the 2020 lockdown in Europe by an observationally constrained regional model using TROPOMI. Atmospheric Chemistry and Physics, 2021, 21, 18227-18245.	4.9	25
124	<title>Scanning imaging absorption spectrometer for atmospheric chartography</title> .,1991,,.		24
125	<title>Retrieval and molecule sensitivity studies for the global ozone monitoring experiment and the scanning imaging absorption spectrometer for atmospheric chartography</title> ., 1991, 1491, 151.		24
126	An overview of the nadir sensor and algorithms for the NPOESS ozone mapping and profiler suite (OMPS). , 2003, , .		24

8

#	Article	IF	CITATIONS
127	Observation of ozone enhancement in the lower troposphere over East Asia from a space-borne ultraviolet spectrometer. Atmospheric Chemistry and Physics, 2015, 15, 9865-9881.	4.9	24
128	Characterization of the OCO-2 instrument line shape functions using on-orbit solar measurements. Atmospheric Measurement Techniques, 2017, 10, 939-953.	3.1	24
129	The added value of a visible channel to a geostationary thermal infrared instrument to monitor ozone for air quality. Atmospheric Measurement Techniques, 2014, 7, 2185-2201.	3.1	23
130	Link Between Arctic Tropospheric BrO Explosion Observed From Space and Seaâ€Salt Aerosols From Blowing Snow Investigated Using Ozone Monitoring Instrument BrO Data and GEOSâ€5 Data Assimilation System. Journal of Geophysical Research D: Atmospheres, 2018, 123, 6954-6983.	3.3	23
131	A geostationary thermal infrared sensor to monitor the lowermost troposphere: O ₃ and CO retrieval studies. Atmospheric Measurement Techniques, 2011, 4, 297-317.	3.1	22
132	Interpreting satellite column observations of formaldehyde over tropical South America. Philosophical Transactions Series A, Mathematical, Physical, and Engineering Sciences, 2007, 365, 1741-1751.	3.4	21
133	Validation of satellite formaldehyde (HCHO) retrievals using observations from 12 aircraft campaigns. Atmospheric Chemistry and Physics, 2020, 20, 12329-12345.	4.9	21
134	Validation of 10-year SAO OMI ozone profile (PROFOZ) product using Aura MLS measurements. Atmospheric Measurement Techniques, 2018, 11, 17-32.	3.1	20
135	Reevaluating the Use of O ₂ Â <i>a</i> ¹ Δ _{<i>g</i>} Band in Spaceborne Remote Sensing of Greenhouse Gases. Geophysical Research Letters, 2018, 45, 5779-5787.	4.0	19
136	Evaluating AURA/OMI ozone profiles using ozonesonde data and EPA surface measurements for August 2006. Atmospheric Environment, 2011, 45, 5523-5530.	4.1	18
137	The impact of using different ozone cross sections on ozone profile retrievals from OMI UV measurements. Journal of Quantitative Spectroscopy and Radiative Transfer, 2013, 130, 365-372.	2.3	18
138	Sensitivity of formaldehyde (HCHO) column measurements from a geostationary satellite to temporal variation of the air mass factor in East Asia. Atmospheric Chemistry and Physics, 2017, 17, 4673-4686.	4.9	18
139	Ozone Monitoring Instrument (OMI) Total Column Water Vapor version 4 validation and applications. Atmospheric Measurement Techniques, 2019, 12, 5183-5199.	3.1	18
140	Dynamical and chemical features of a cutoff low over northeast China in July 2007: Results from satellite measurements and reanalysis. Advances in Atmospheric Sciences, 2013, 30, 525-540.	4.3	17
141	Validation and update of OMI Total Column Water Vapor product. Atmospheric Chemistry and Physics, 2016, 16, 11379-11393.	4.9	17
142	A semi-empirical potential energy surface and line list for H ₂ ¹⁶ O extending into the near-ultraviolet. Atmospheric Chemistry and Physics, 2020, 20, 10015-10027.	4.9	17
143	Cloud retrieval algorithm for the European Space Agency's Global Ozone Monitoring Experiment. , 1998, , .		16
144	Dynamic formation of extreme ozone minimum events over the Tibetan Plateau during northern winters 1987–2001. Journal of Geophysical Research, 2010, 115, .	3.3	16

#	Article	IF	CITATIONS
145	Estimating the influence of lightning on upper tropospheric ozone using NLDN lightning data and CMAQ model. Atmospheric Environment, 2013, 67, 219-228.	4.1	16
146	The GeoTASO airborne spectrometer project. Proceedings of SPIE, 2014, , .	0.8	16
147	Description of a formaldehyde retrieval algorithm for the Geostationary Environment Monitoring Spectrometer (GEMS). Atmospheric Measurement Techniques, 2019, 12, 3551-3571.	3.1	16
148	Towards a satellite formaldehyde – in situ hybrid estimate for organic aerosol abundance. Atmospheric Chemistry and Physics, 2019, 19, 2765-2785.	4.9	15
149	Pressure Broadening of the 2.4978-THz Rotational Lines of HO2 by N2 and O2. Journal of Molecular Spectroscopy, 1994, 163, 67-70.	1.2	14
150	TEMPO Green Paper: Chemistry, physics, and meteorology experiments with the Tropospheric Emissions: monitoring of pollution instrument. , 2019, , .		14
151	An ozone depletion event in the sub-arctic surface layer over Hudson Bay, Canada. Journal of Atmospheric Chemistry, 2007, 57, 255-280.	3.2	13
152	A climatology of visible surface reflectance spectra. Journal of Quantitative Spectroscopy and Radiative Transfer, 2016, 180, 39-46.	2.3	13
153	Deriving the slit functions from OMI solar observations and its implications for ozone-profile retrieval. Atmospheric Measurement Techniques, 2017, 10, 3677-3695.	3.1	13
154	Ultraviolet and visible spectroscopy and spaceborne remote sensing of the Earth's atmosphere. Comptes Rendus Physique, 2005, 6, 836-847.	0.9	12
155	Mapping tropospheric ozone profiles from an airborne ultraviolet-visible spectrometer. Applied Optics, 2005, 44, 3312.	2.1	12
156	Cross-evaluation of GEMS tropospheric ozone retrieval performance using OMI data and the use of an ozonesonde dataset over East Asia for validation. Atmospheric Measurement Techniques, 2019, 12, 5201-5215.	3.1	12
157	Explicit Aerosol Correction of OMI Formaldehyde Retrievals. Earth and Space Science, 2019, 6, 2087-2105.	2.6	11
158	Spectral calibration of the MethaneAIR instrument. Atmospheric Measurement Techniques, 2021, 14, 3737-3753.	3.1	11
159	Spectroscopic Measurements of Tropospheric Composition from Satellite Measurements in the Ultraviolet and Visible: Steps Toward Continuous Pollution Monitoring from Space. , 2006, , 1-25.		10
160	Spatiotemporal Variation in Tropospheric Column Ozone over East Asia Observed by GOME and Ozonesondes. Scientific Online Letters on the Atmosphere, 2008, 4, 117-120.	1.4	10
161	Dealing with spatial heterogeneity in pointwise-to-gridded- data comparisons. Atmospheric Measurement Techniques, 2022, 15, 41-59.	3.1	10
162	Response of Hurricane Harvey's rainfall to anthropogenic aerosols: A sensitivity study based on spectral bin microphysics with simulated aerosols. Atmospheric Research, 2020, 242, 104965.	4.1	9

#	Article	IF	CITATIONS
163	Enhanced Mid-Latitude Tropospheric Column Ozone over East Asia: Coupled Effects of Stratospheric Ozone Intrusion and Anthropogenic Sources. Journal of the Meteorological Society of Japan, 2012, 90, 207-222.	1.8	9
164	New retrieval of BrO from SCIAMACHY limb: an estimate of the stratospheric bromine loading during April 2008. Atmospheric Measurement Techniques, 2013, 6, 2549-2561.	3.1	8
165	Tropospheric ozone profiles from a ground-based ultraviolet spectrometer: a new retrieval method. Applied Optics, 2006, 45, 2352.	2.1	6
166	Linearization of the effect of slit function changes for improving Ozone Monitoring Instrument ozone profile retrievals. Atmospheric Measurement Techniques, 2019, 12, 3777-3788.	3.1	6
167	OMI total bromine monoxide (OMBRO) data product: algorithm, retrieval and measurement comparisons. Atmospheric Measurement Techniques, 2019, 12, 2067-2084.	3.1	6
168	Revolutionary Air-Pollution Applications from Future Tropospheric Emissions: Monitoring of Pollution (TEMPO) Observations. Bulletin of the American Meteorological Society, 2021, 102, E1735-E1741.	3.3	6
169	Impact of using a new ultraviolet ozone absorption cross-section dataset on OMI ozone profile retrievals. Atmospheric Measurement Techniques, 2020, 13, 5845-5854.	3.1	6
170	Improvement of OMI ozone profile retrievals by simultaneously fitting polar mesospheric clouds. Atmospheric Measurement Techniques, 2016, 9, 4521-4531.	3.1	6
171	Quantifying the Impact of Excess Moisture From Transpiration From Crops on an Extreme Heat Wave Event in the Midwestern U.S.: A Topâ€Down Constraint From Moderate Resolution Imaging Spectroradiometer Water Vapor Retrieval. Journal of Geophysical Research D: Atmospheres, 2020, 125, e2019ID031941.	3.3	5
172	<title>Polar stratospheric cloud detection from the ILAS instrument</title> ., 2001, 4150, 68.		4
173	Analysis of ACAM Data for Trace Gas Retrievals during the 2011 DISCOVER-AQ Campaign. Journal of Spectroscopy, 2015, 2015, 1-7.	1.3	4
174	A precise photometric ratio via laser excitation of the sodium layer – II. Two-photon excitation using lasers detuned from 589.16 and 819.71Ânm resonances. Monthly Notices of the Royal Astronomical Society, 2021, 508, 4412-4428.	4.4	4
175	A precise photometric ratio via laser excitation of the sodium layer – I. One-photon excitation using 342.78Ânm light. Monthly Notices of the Royal Astronomical Society, 2021, 508, 4399-4411.	4.4	4
176	From Radiation Fields to Atmospheric Concentrations – Retrieval of Geophysical Parameters. , 2011, , 99-127.		3
177	Radiative transfer acceleration based on the principal component analysis and lookup table of corrections: optimization and application to UV ozone profile retrievals. Atmospheric Measurement Techniques, 2021, 14, 2659-2672.	3.1	3
178	Validation and Comparison of Tropospheric Column Ozone Derived from GOME Measurements with Ozonesondes over Japan. Scientific Online Letters on the Atmosphere, 2007, 3, 41-44.	1.4	3
179	Far-infrared spectroscopy of the earth's stratosphere. , 1985, , .		2
180	Impact of Using a New High-Resolution Solar Reference Spectrum on OMI Ozone Profile Retrievals. Remote Sensing, 2022, 14, 37.	4.0	2

#	Article	IF	CITATIONS
181	Evaluation of the Stratospheric and Tropospheric Bromine Burden Over Fairbanks, Alaska Based on Column Retrievals of Bromine Monoxide. Journal of Geophysical Research D: Atmospheres, 2021, 126, e2020JD032896.	3.3	1
182	Atmospheric trace gas measurements from the European Space Agency's Global Ozone Monitoring Experiment. , 1998, , .		0
183	<title>Tropospheric formaldehyde measurements from the ESA GOME instrument</title> ., 2001, 4150, 1.		0
184	Determination of Density at High Altitudes Using Rayleigh and Raman Scattering of Solar Radiation. , 2005, , .		0
185	An Airborne Spectrometer and Retrieval Development Project for Air Quality Measurements. , 2011, , .		0
186	A Geostationary air quality monitor for the Middle East. Journal of Physics: Conference Series, 2017, 869, 012085.	0.4	0
187	Global Monitoring of Tropospheric Pollution from Geostationary Orbit. , 2007, , .		0
188	High spatial and temporal resolution estimates of air pollutants from the TEMPO satellite: Methodological opportunities and challenges for environmental epidemiology studies. ISEE Conference Abstracts, 2020, 2020, .	0.0	0
189	An optimal estimation-based retrieval of upper atmospheric oxygen airglow and temperature from SCIAMACHY limb observations. Atmospheric Measurement Techniques, 2022, 15, 3721-3745.	3.1	0